Unsupervised Physics-Informed Super-Resolution of Strong Lensing Images for Sparse Datasets

Anirudh Shankar
Université de Strasbourg, CNRS, Observatoire astronomique de Strasbourg,
UMR 7550, F-67000 Strasbourg, France
anirudh.shankar@astro.unistra.fr

Michael W. Toomey
Center for Theoretical Physics, Massachusetts Institute of Technology,
Cambridge, MA 02139, USA
mtoomey@mit.edu

Sergei Gleyzer
Department of Physics & Astronomy, University of Alabama,
Tuscaloosa, AL 35401, USA
sgleyzer@ua.edu

Abstract

Strong gravitational lensing has emerged as a powerful method for probing the nature of dark matter via substructure within galaxies. However, the limited availability of high-quality, high-resolution lensing images poses significant challenges to developing robust machine learning models, particularly for super-resolution imaging tasks. In this work, we present a novel, physics-informed approach to super-resolution of strong lensing images, designed specifically for sparse datasets. Unlike traditional supervised methods, our approach is fully unsupervised, requiring no ground-truth high-resolution images for training. By incorporating the gravitational lens equation directly into the architecture, our model is capable of extracting key physical information about the lens system, such as the distribution of dark matter in the lensing system, more efficiently in addition to enhancing image resolution. We validate our approach on simulated lensing datasets, demonstrating that our method not only improves image clarity but also provides meaningful insights into dark matter substructure. This work paves the way for more efficient analysis of upcoming large-scale surveys, including those from LSST and Euclid, which will dramatically expand the available data for strong lensing studies.

1 Introduction

Strong gravitational lensing has proven to be one of the most valuable tools in modern astrophysics for probing the distribution of dark matter (DM) [16, 4, 22, 21, 19, 11], particularly through the substructure within dark matter halos [9, 6, 10, 5, 18, 13]. In particular, the distortion and magnification of background galaxies provide unique insights into the gravitational potential of the intervening lensing galaxy and its surrounding dark matter [1, 8, 23, 3, 14]. However, the extraction of meaningful information from these images is often hindered by a number of challenges, including limited datasets and the inherent complexity of modeling the lensing effect.

38th Conference on Neural Information Processing Systems (NeurIPS 2024).

Traditional approaches to studying strong lensing rely heavily on large, labeled datasets that require ground-truth high-resolution (HR) images. However, due to the rarity of these cosmic alignments, only a small number of strong lensing events have been observed, severely limiting the availability of high-quality HR datasets. This scarcity poses significant challenges to training supervised machine learning models, particularly in the context of super-resolution (SR) imaging, where reconstructing fine details from low-resolution (LR) images is critical.

In response to these challenges, we propose a novel, physics-informed approach to super-resolution imaging for strong gravitational lensing that leverages unsupervised learning methods. Our model does not require HR ground truths for training and instead incorporates the physics of gravitational lensing directly into the architecture. By embedding the lens equation into the learning process, the model not only enhances image resolution but also extracts key information about the lens system, such as the deflection angle and the underlying mass distribution of dark matter. The novelty of our approach is that by including the lens equation directly into our architecture, it does not have to be *learned* during training.

This approach has the potential to revolutionize the analysis of strong lensing datasets, particularly as upcoming surveys, such as Euclid [17, 12] and the Legacy Survey of Space and Time (LSST; [20]), are expected to deliver an unprecedented volume of lensing images. By addressing the current limitations imposed by sparse datasets and unsupervised learning, our work offers a robust framework for improving image resolution and gaining further insight into the nature of dark matter.

2 Data and methods

2.1 Datasets

For this study, we use simulated galaxy-galaxy strong lensing images that closely resemble data from real experiments. They represent a mock instrument with point-spread function $\sim$, and two that represent mock observation with Euclid and the Hubble Space Telescope (HST). To distinguish the datasets we refer to them as Model 1, 2, and 3 respectively. Given the scarcity of observed lensing events and the challenges posed by limited real-world data, simulations have become a crucial resource for developing and testing machine learning models, especially for lensing systems.

We describe the datasets as 'sparse' due to two reasons: they contain no labelled data, i.e., no high-resolution representations to train from, and due to the small training sample size of 1024 images per dataset. By incorporating the physics of strong gravitational lensing into our model, we achieve super-resolution despite these limitations. These images were generated using the publicly available `lenstronomy` code, which models both the source and lens galaxies. The source galaxy is assumed to follow a Sérsic light profile, a commonly used analytic model to describe the intensity distribution of galaxies.

For the lensing galaxy, we implemented a Singular Isothermal Sphere (SIS) model for the dark matter halo, consistent with the standard cold dark matter (CDM) paradigm. The lensing effect was simulated by applying relativistic distortion to the source galaxy's image, creating the characteristic arcs and Einstein rings observed in strong lensing events. In addition, we have simulated the images with three different choice of substructure: no substructure, CDM-like substructure, and axion dark matter substructure. For more details on constructing these data sets the reader should consult [2].

The dataset includes both low-resolution (LR) images, which serve as input to the model, and corresponding high-resolution (HR) images for evaluation. However, during the training process, the model operates in a completely unsupervised manner, without access to the HR images, making it a true test of its ability to extract fine details from sparse datasets.

2.2 Motivation

Strong gravitational lensing, as illustrated in Figure 1, can be described by the strong lensing equation as follows:

$$\overrightarrow{I} = \overrightarrow{S} + \overrightarrow{\alpha}(x, y) \tag{1}$$

Where the deflection angle, $\overrightarrow{\alpha}$, a property of the lens relating to its mass distribution, directs the mapping of positions between the source light profile $\overrightarrow{S}$ (usually a galaxy) and the lensing image $\overrightarrow{I}$.

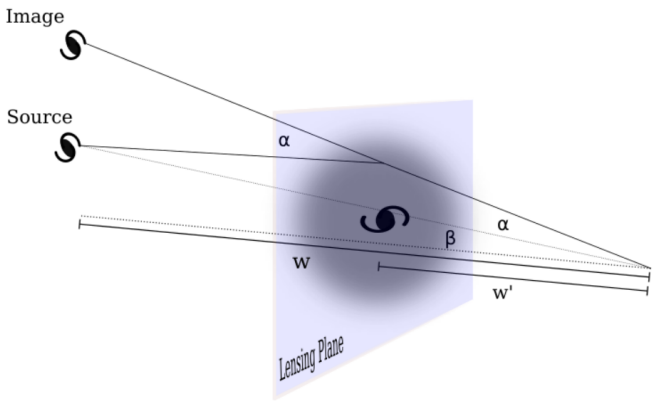

Figure 1: The geometry of a strong lensing system with background galaxy, lensing dark matter halo, and observer, from left to right. The galaxy labeled *Image* represents the perceived location of the true galaxy position *Source* due to a deflection by the dark matter halo by $\vec{\alpha}$.

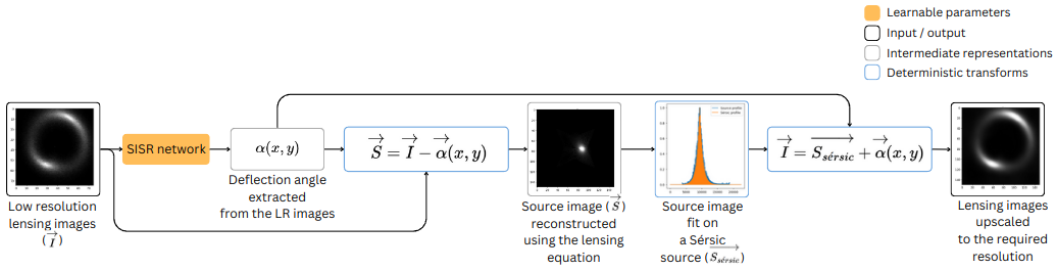

Figure 2: Physics-informed super-resolution model schematic

With the deflection angle and a known source profile, we can very easily create lensing images at any resolution, which is the principle our work is based on. For this purpose, we use the Sérsic profile, a good approximation of a galaxy's light profile [7] [24].

2.3 Model architecture

We present a Physics-Informed architecture that uses the physics of strong gravitational lensing in the unsupervised training of a super-resolution network. Figure 2 presents the model's construction. A single-image super-resolution convolutional neural network (SISR CNN) is used to extract deflection angle representations at the required resolution from the lensing images. The network is constructed to deliver representations at the required resolution using sub-pixel convolution layers, and is constructed with residual connections [15]. The extracted deflection angle is used in the lensing equation to reconstruct the source image, which is then fit on the Sérsic profile. The Sérsic profile, along with the earlier extracted deflection angle in the lensing equation is used to produce up-scaled lensing images. Using the deflection angle to obtain the Sérsic source as a continuous mathematical function is what enables the up-scaling of the lensing images to any required resolution, in an unsupervised manner. Training is preformed 'indirectly' through the imposition of several physical and mathematical constraints, as described in the following section.

2.4 Losses and constraints

Multi-scale loss Super-resolution inherently requires the characteristics of the low-resolution images to be preserved when up-scaling. This property is used as a constraint, which is imposed on different image scales: in the dimensions of the input images, in the dimensions of the output super-resolution images and, on a downscaled version of the lensing images.
The constraints that follow are imposed on many of the described image scales.

Mean squared error (MSE) The MSE between the regenerated source images and the Sérsic profile, and the MSE between the input lensing images and the re-lensed output images are used as constraints. This guides training of the CNN to produce the deflection angle.

Variation density (VD) loss This quantity measures the the total change the deflection angle undergoes in both x and y directions, normalized by image size. It is essentially a smoothness constraint, aimed at ensuring the deflection angle is devoid of extreme-valued artifacts, and rather stays fairly continuous. A weight is attached to this loss as a coefficient, to control the permitted variation amount. This helps ensuring meaningful convergence, as the MSEs described earlier are often not sufficient by themselves.

3 Results & Discussion

We evaluate the model's performance by comparing the super-resolved (SR) images with separately simulated high resolution (HR) images. The three metrics used are the MSE between the SR and the HR images, the Structural Similarity Index Measure (SSIM), and the Peak Signal-to-Noise Ratio (PSNR). Table 1 contains the sub-structure wise results of our model.

Table 1: Sub-structure-wise results of the Physics-Informed training

Dataset	Sub-structure	MSE	SSIM	PSNR
Model-1	No sub-structure	0.00500	0.720	23.508
	Axion DM (vortex)	0.00291	0.768	25.906
	CDM (sub-halo)	0.00364	0.748	24.988
Model-2	No sub-structure	0.00237	0.223	26.396
	Axion DM (vortex)	0.00272	0.214	25.812
	CDM (sub-halo)	0.00264	0.216	25.932
Model-3	No sub-structure	0.00199	0.732	27.356
	Axion DM (vortex)	0.00244	0.715	26.463
	CDM (sub-halo)	0.00232	0.715	26.683

Lower SSIM scores in the Model-2 dataset Model 2, which represents a mock Euclid-like detector, has a significantly lower PSF compared to Model 1 and Model 3 (which mimic a fake detector and the Hubble Space Telescope, respectively). The lower PSF in the Euclid-mock dataset causes broader and more blurred features in the observed images, making it harder for the model to distinguish fine details. This results in reduced SSIM scores, as the model struggles to accurately reconstruct high-resolution images from less detailed, blurred inputs. In contrast, Model 3 (HST-like) benefits from a higher PSF, capturing sharper, more distinct features that allow for better super-resolution performance. Similarly, Model 1, while synthetic, was designed to have a PSF similar to HST, explaining its comparable performance. Thus, the poorer results for Model 2 can largely be attributed to the limitations imposed by the lower PSF in the mock Euclid data.

Training sensitivity to the VD loss It was observed that meaningful convergence during training depended on the weights of the VD loss. Weights that are too small do not bring the required smoothness in the deflection angle, while ones that are too large cause over-smoothing, limiting the model from producing accurate deflection angles. The accuracy of the deflection angle guides the reconstruction of the source image and the eventual super-resolution of the lensing images. Inaccuracies produced can magnify through the pipeline, and to arrive at an optimal selection for the VD loss weights, a Bayesian optimization pipeline or a decaying weight approach can be used.

Qualitative estimation of errors Errors in the described architecture can arise from two sources: (1) the accuracy limitation of the SISR CNN used in extracting the deflection angles and (2) the accuracy in the estimation of the source representation by the Sérsic profile. For lensing images produced with more complex sources that cannot be accurately captured by a Sérsic profile, super-resolution of the lensing images through this pipeline may bring inaccuracies and difficulty in ensuring convergence.

Application to real images Real images either being images of real lensing systems or being lensing images simulated using real galaxy images can be analyzed by this architecture. The performance of the model on such images however is dependent on the accurate reconstruction of the source images by the Sérsic profile. To ensure better approximation, a combination of Sérsic profiles can be employed.

In summary, this work introduces a physics-informed, unsupervised approach to super-resolving strong gravitational lensing images, addressing the challenges posed by sparse datasets. By embedding the physics of strong gravitational lensing into the neural network architecture, our method provides improved image quality and model performance while preserving critical information about dark matter substructure. The model's performance across multiple datasets, particularly for varying instrument characteristics, highlights its adaptability and robustness. Moving forward, this approach holds significant promise for future large-scale surveys like Euclid and VRO, where high volumes of lensing data will become available. By refining the resolution of lensing data, our model sets the stage for more detailed studies into the nature of dark matter, paving the way for new discoveries in fundamental physics. Further improvements, particularly in handling diverse lensing conditions and noise characteristics, will enhance its applicability across a wider range of observational data.

Acknowledgements

A.S. was a participant in the Google Summer of Code 2024 program. S.G. was supported in part by U.S. National Science Foundation award No. 2108645. Portions of this work were conducted in MIT's Center for Theoretical Physics and partially supported by the U.S. Department of Energy under grant Contract Number DE-SC0012567. M.W.T. acknowledges financial support from the Simons Foundation (Grant Number 929255).

References

[1] S. Alexander, S. Gleyzer, E. McDonough, M. W. Toomey, and E. Usai. Deep Learning the Morphology of Dark Matter Substructure. , 893(1):15, Apr. 2020. doi: 10.3847/1538-4357/ab7925.

[2] S. Alexander, S. Gleyzer, H. Parul, P. Reddy, M. Tidball, and M. W. Toomey. Domain Adaptation for Simulation-based Dark Matter Searches with Strong Gravitational Lensing. *Astrophys. J.*, 954(1):28, 2023. doi: 10.3847/1538-4357/acdfc7.

[3] N. Anau Montel, A. Coogan, C. Correa, K. Karchev, and C. Weniger. Estimating the warm dark matter mass from strong lensing images with truncated marginal neural ratio estimation. , 518(2):2746–2760, Jan. 2023. doi: 10.1093/mnras/stac3215.

[4] M. Barnabè, O. Czoske, L. V. E. Koopmans, T. Treu, and A. S. Bolton. Two-dimensional kinematics of SLACS lenses - III. Mass structure and dynamics of early-type lens galaxies beyond z 0.1. , 415(3):2215–2232, Aug. 2011. doi: 10.1111/j.1365-2966.2011.18842.x.

[5] D. Bayer, L. V. E. Koopmans, J. P. McKean, S. Vegetti, T. Treu, C. D. Fassnacht, and K. Glazebrook. Probing sub-galactic mass structure with the power spectrum of surface-brightness anomalies in high-resolution observations of galaxy-galaxy strong gravitational lenses - I. Power-spectrum measurement and feasibility study. , 523(1):1326–1345, July 2023. doi: 10.1093/mnras/stad1403.

[6] J. Brehmer, S. Mishra-Sharma, J. Hermans, G. Louppe, and K. Cranmer. Mining for Dark Matter Substructure: Inferring Subhalo Population Properties from Strong Lenses with Machine Learning. , 886(1):49, Nov. 2019. doi: 10.3847/1538-4357/ab4c41.

[7] N. Caon, M. Capaccioli, and M. D'Onofrio. On the shape of the light profiles of early-type galaxies. *Monthly Notices of the Royal Astronomical Society*, 265(4):1013–1021, 1993.

[8] A. Ç. Şengül and C. Dvorkin. Probing dark matter with strong gravitational lensing through an effective density slope. , 516(1):336–357, Oct. 2022. doi: 10.1093/mnras/stac2256.

[9] T. Daylan, F.-Y. Cyr-Racine, A. Diaz Rivero, C. Dvorkin, and D. P. Finkbeiner. Probing the Small-scale Structure in Strongly Lensed Systems via Transdimensional Inference. , 854(2): 141, Feb. 2018. doi: 10.3847/1538-4357/aaaa1e.

[10] A. Diaz Rivero and C. Dvorkin. Direct detection of dark matter substructure in strong lens images with convolutional neural networks. , 101(2):023515, Jan. 2020. doi: 10.1103/PhysRevD.101.023515.

[11] A. Etherington, J. W. Nightingale, R. Massey, A. Robertson, X. Cao, A. Amvrosiadis, S. Cole, C. S. Frenk, Q. He, D. J. Lagattuta, S. Lange, and R. Li. Beyond the bulge-halo conspiracy? Density profiles of early-type galaxies from extended-source strong lensing. , 521(4):6005–6018, June 2023. doi: 10.1093/mnras/stad582.

[12] Euclid Collaboration, R. Scaramella, J. Amiaux, Y. Mellier, C. Burigana, C. S. Carvalho, J. C. Cuillandre, A. Da Silva, A. Derosa, J. Dinis, E. Maiorano, M. Maris, I. Tereno, R. Laureijs, T. Boenke, G. Buenadicha, X. Dupac, L. M. Gaspar Venancio, P. Gómez-Álvarez, J. Hoar, J. Lorenzo Alvarez, G. D. Racca, G. Saavedra-Criado, J. Schwartz, R. Vavrek, M. Schirmer, H. Aussel, R. Azzollini, V. F. Cardone, M. Cropper, A. Ealet, B. Garilli, W. Gillard, B. R. Granett, L. Guzzo, H. Hoekstra, K. Jahnke, T. Kitching, T. Maciaszek, M. Meneghetti, L. Miller, R. Nakajima, S. M. Niemi, F. Pasian, W. J. Percival, S. Pottinger, M. Sauvage, M. Scodeggio, S. Wachter, A. Zacchei, N. Aghanim, A. Amara, T. Auphan, N. Auricchio, S. Awan, A. Balestra, R. Bender, C. Bodendorf, D. Bonino, E. Branchini, S. Brau-Nogue, M. Brescia, G. P. Candini, V. Capobianco, C. Carbone, R. G. Carlberg, J. Carretero, R. Casas, F. J. Castander, M. Castellano, S. Cavuoti, A. Cimatti, R. Cledassou, G. Congedo, C. J. Conselice, L. Conversi, Y. Copin, L. Corcione, A. Costille, F. Courbin, H. Degaudenzi, M. Douspis, F. Dubath, C. A. J. Duncan, S. Dusini, S. Farrens, S. Ferriol, P. Fosalba, N. Fourmanoit, M. Frailis, E. Franceschi, P. Franzetti, M. Fumana, B. Gillis, C. Giocoli, A. Grazian, F. Grupp, S. V. H. Haugan, W. Holmes, F. Hormuth, P. Hudelot, S. Kermiche, A. Kiessling, M. Kilbinger, R. Kohley, B. Kubik, M. Kümmel, M. Kunz, H. Kurki-Suonio, O. Lahav, S. Ligori, P. B. Lilje, I. Lloro, O. Mansutti, O. Marggraf, K. Markovic, F. Marulli, R. Massey, S. Maurogordato, M. Melchior, E. Merlin, G. Meylan, J. J. Mohr, M. Moresco, B. Morin, L. Moscardini, E. Munari, R. C. Nichol, C. Padilla, S. Paltani, J. Peacock, K. Pedersen, V. Pettorino, S. Pires, M. Poncet, L. Popa, L. Pozzetti, F. Raison, R. Rebolo, J. Rhodes, H. W. Rix, M. Roncarelli, E. Rossetti, R. Saglia, P. Schneider, T. Schrabback, A. Secroun, G. Seidel, S. Serrano, C. Sirignano, G. Sirri, J. Skottfelt, L. Stanco, J. L. Starck, P. Tallada-Crespí, D. Tavagnacco, A. N. Taylor, H. I. Teplitz, R. Toledo-Moreo, F. Torradeflot, M. Trifoglio, E. A. Valentijn, L. Valenziano, G. A. Verdoes Kleijn, Y. Wang, N. Welikala, J. Weller, M. Wetzstein, G. Zamorani, J. Zoubian, S. Andreon, M. Baldi, S. Bardelli, A. Boucaud, S. Camera, D. Di Ferdinando, G. Fabbian, R. Farinelli, S. Galeotta, J. Graciá-Carpio, D. Maino, E. Medinaceli, S. Mei, C. Neissner, G. Polenta, A. Renzi, E. Romelli, C. Rosset, F. Sureau, M. Tenti, T. Vassallo, E. Zucca, C. Baccigalupi, A. Balaguera-Antolínez, P. Battaglia, A. Biviano, S. Borgani, E. Bozzo, R. Cabanac, A. Cappi, S. Casas, G. Castignani, C. Colodro-Conde, J. Coupon, H. M. Courtois, J. Cuby, S. de la Torre, S. Desai, H. Dole, M. Fabricius, M. Farina, P. G. Ferreira, F. Finelli, P. Flose-Reimberg, S. Fotopoulou, K. Ganga, G. Gozaliasl, I. M. Hook, E. Keihanen, C. C. Kirkpatrick, P. Liebing, V. Lindholm, G. Mainetti, M. Martinelli, N. Martinet, M. Maturi, H. J. McCracken, R. B. Metcalf, G. Morgante, J. Nightingale, A. Nucita, L. Patrizii, D. Potter, G. Riccio, A. G. Sánchez, D. Sapone, J. A. Schewtschenko, M. Schultheis, V. Scottez, R. Teyssier, I. Tutusaus, J. Valiviita, M. Viel, W. Vriend, and L. Whittaker. Euclid preparation. I. The Euclid Wide Survey. , 662:A112, June 2022. doi: 10.1051/0004-6361/202141938.

[13] D. Gilman, S. Birrer, T. Treu, C. R. Keeton, and A. Nierenberg. Probing the nature of dark matter by forward modelling flux ratios in strong gravitational lenses. , 481(1):819–834, Nov. 2018. doi: 10.1093/mnras/sty2261.

[14] D. Gilman, Y.-M. Zhong, and J. Bovy. Constraining resonant dark matter self-interactions with strong gravitational lenses. , 107(10):103008, May 2023. doi: 10.1103/PhysRevD.107.103008.

[15] K. He, X. Zhang, S. Ren, and J. Sun. Deep residual learning for image recognition. In *Proceedings of the IEEE conference on computer vision and pattern recognition*, pages 770–778, 2016.

[16] L. V. E. Koopmans, A. Bolton, T. Treu, O. Czoske, M. W. Auger, M. Barnabè, S. Vegetti, R. Gavazzi, L. A. Moustakas, and S. Burles. The Structure and Dynamics of Massive Early-Type Galaxies: On Homology, Isothermality, and Isotropy Inside One Effective Radius. , 703 (1):L51–L54, Sept. 2009. doi: 10.1088/0004-637X/703/1/L51.

[17] R. Laureijs, J. Amiaux, S. Arduini, J. L. Augueres, J. Brinchmann, R. Cole, M. Cropper, C. Dabin, L. Duvet, A. Ealet, B. Garilli, P. Gondoin, L. Guzzo, J. Hoar, H. Hoekstra, R. Holmes, T. Kitching, T. Maciaszek, Y. Mellier, F. Pasian, W. Percival, J. Rhodes, G. Saavedra Criado, M. Sauvage, R. Scaramella, L. Valenziano, S. Warren, R. Bender, F. Castander, A. Cimatti, O. Le Fèvre, H. Kurki-Suonio, M. Levi, P. Lilje, G. Meylan, R. Nichol, K. Pedersen, V. Popa, R. Rebolo Lopez, H. W. Rix, H. Rottgering, W. Zeilinger, F. Grupp, P. Hudelot, R. Massey, M. Meneghetti, L. Miller, S. Paltani, S. Paulin-Henriksson, S. Pires, C. Saxton, T. Schrabback, G. Seidel, J. Walsh, N. Aghanim, L. Amendola, J. Bartlett, C. Baccigalupi, J. P. Beaulieu, K. Benabed, J. G. Cuby, D. Elbaz, P. Fosalba, G. Gavazzi, A. Helmi, I. Hook, M. Irwin, J. P. Kneib, M. Kunz, F. Mannucci, L. Moscardini, C. Tao, R. Teyssier, J. Weller, G. Zamorani, M. R. Zapatero Osorio, O. Boulade, J. J. Foumond, A. Di Giorgio, P. Guttridge, A. James, M. Kemp, J. Martignac, A. Spencer, D. Walton, T. Blümchen, C. Bonoli, F. Bortoletto, C. Cerna, L. Corcione, C. Fabron, K. Jahnke, S. Ligori, F. Madrid, L. Martin, G. Morgante, T. Pamplona, E. Prieto, M. Riva, R. Toledo, M. Trifoglio, F. Zerbi, F. Abdalla, M. Douspis, C. Grenet, S. Borgani, R. Bouwens, F. Courbin, J. M. Delouis, P. Dubath, A. Fontana, M. Frailis, A. Grazian, J. Koppenhöfer, O. Mansutti, M. Melchior, M. Mignoli, J. Mohr, C. Neissner, K. Noddle, M. Poncet, M. Scodeggio, S. Serrano, N. Shane, J. L. Starck, C. Surace, A. Taylor, G. Verdoes-Kleijn, C. Vuerli, O. R. Williams, A. Zacchei, B. Altieri, I. Escudero Sanz, R. Kohley, T. Oosterbroek, P. Astier, D. Bacon, S. Bardelli, C. Baugh, F. Bellagamba, C. Benoist, D. Bianchi, A. Biviano, E. Branchini, C. Carbone, V. Cardone, D. Clements, S. Colombi, C. Conselice, G. Cresci, N. Deacon, J. Dunlop, C. Fedeli, F. Fontanot, P. Franzetti, C. Giocoli, J. Garcia-Bellido, J. Gow, A. Heavens, P. Hewett, C. Heymans, A. Holland, Z. Huang, O. Ilbert, B. Joachimi, E. Jennins, E. Kerins, A. Kiessling, D. Kirk, R. Kotak, O. Krause, O. Lahav, F. van Leeuwen, J. Lesgourgues, M. Lombardi, M. Magliocchetti, K. Maguire, E. Majerotto, R. Maoli, F. Marulli, S. Maurogordato, H. McCracken, R. McLure, A. Melchiorri, A. Merson, M. Moresco, M. Nonino, P. Norberg, J. Peacock, R. Pello, M. Penny, V. Pettorino, C. Di Porto, L. Pozzetti, C. Quercellini, M. Radovich, A. Rassat, N. Roche, S. Ronayette, E. Rossetti, B. Sartoris, P. Schneider, E. Semboloni, S. Serjeant, F. Simpson, C. Skordis, G. Smadja, S. Smartt, P. Spano, S. Spiro, M. Sullivan, A. Tilquin, R. Trotta, L. Verde, Y. Wang, G. Williger, G. Zhao, J. Zoubian, and E. Zucca. Euclid Definition Study Report. *arXiv e-prints*, art. arXiv:1110.3193, Oct. 2011. doi: 10.48550/arXiv.1110.3193.

[18] R. Li, C. S. Frenk, S. Cole, L. Gao, S. Bose, and W. A. Hellwing. Constraints on the identity of the dark matter from strong gravitational lenses. , 460(1):363–372, July 2016. doi: 10.1093/mnras/stw939.

[19] R. Li, Y. Shu, and J. Wang. Strong-lensing measurement of the total-mass-density profile out to three effective radii for z $\sim$ 0.5 early-type galaxies. , 480(1):431–438, Oct. 2018. doi: 10.1093/mnras/sty1813.

[20] LSST Science Collaboration, P. A. Abell, J. Allison, S. F. Anderson, J. R. Andrew, J. R. P. Angel, L. Armus, D. Arnett, S. J. Asztalos, T. S. Axelrod, S. Bailey, D. R. Ballantyne, J. R. Bankert, W. A. Barkhouse, J. D. Barr, L. F. Barrientos, A. J. Barth, J. G. Bartlett, A. C. Becker, J. Becla, T. C. Beers, J. P. Bernstein, R. Biswas, M. R. Blanton, J. S. Bloom, J. J. Bochanski, P. Boeshaar, K. D. Borne, M. Bradac, W. N. Brandt, C. R. Bridge, M. E. Brown, R. J. Brunner, J. S. Bullock, A. J. Burgasser, J. H. Burge, D. L. Burke, P. A. Cargile, S. Chandrasekharan, G. Chartas, S. R. Chesley, Y.-H. Chu, D. Cinabro, M. W. Claire, C. F. Claver, D. Clowe, A. J. Connolly, K. H. Cook, J. Cooke, A. Cooray, K. R. Covey, C. S. Culliton, R. de Jong, W. H. de Vries, V. P. Debattista, F. Delgado, I. P. Dell'Antonio, S. Dhital, R. Di Stefano, M. Dickinson, B. Dilday, S. G. Djorgovski, G. Dobler, C. Donalek, G. Dubois-Felsmann, J. Durech, A. Eliasdottir, M. Eracleous, L. Eyer, E. E. Falco, X. Fan, C. D. Fassnacht, H. C. Ferguson, Y. R. Fernandez, B. D. Fields, D. Finkbeiner, E. E. Figueroa, D. B. Fox, H. Francke, J. S. Frank, J. Frieman, S. Fromenteau, M. Furqan, G. Galaz, A. Gal-Yam, P. Garnavich, E. Gawiser, J. Geary, P. Gee, R. R. Gibson, K. Gilmore, E. A. Grace, R. F. Green, W. J. Gressler, C. J. Grillmair, S. Habib, J. S. Haggerty, M. Hamuy, A. W. Harris, S. L. Hawley, A. F. Heavens, L. Hebb, T. J. Henry,

E. Hileman, E. J. Hilton, K. Hoadley, J. B. Holberg, M. J. Holman, S. B. Howell, L. Infante, Z. Ivezic, S. H. Jacoby, B. Jain, R, Jedicke, M. J. Jee, J. Garrett Jernigan, S. W. Jha, K. V. Johnston, R. L. Jones, M. Juric, M. Kaasalainen, Styliani, Kafka, S. M. Kahn, N. A. Kaib, J. Kalirai, J. Kantor, M. M. Kasliwal, C. R. Keeton, R. Kessler, Z. Knezevic, A. Kowalski, V. L. Krabbendam, K. S. Krughoff, S. Kulkarni, S. Kuhlman, M. Lacy, S. Lepine, M. Liang, A. Lien, P. Lira, K. S. Long, S. Lorenz, J. M. Lotz, R. H. Lupton, J. Lutz, L. M. Macri, A. A. Mahabal, R. Mandelbaum, P. Marshall, M. May, P. M. McGehee, B. T. Meadows, A. Meert, A. Milani, C. J. Miller, M. Miller, D. Mills, D. Minniti, D. Monet, A. S. Mukadam, E. Nakar, D. R. Neill, J. A. Newman, S. Nikolaev, M. Nordby, P. O'Connor, M. Oguri, J. Oliver, S. S. Olivier, J. K. Olsen, K. Olsen, E. W. Olszewski, H. Oluseyi, N. D. Padilla, A. Parker, J. Pepper, J. R. Peterson, C. Petry, P. A. Pinto, J. L. Pizagno, B. Popescu, A. Prsa, V. Radcka, M. J. Raddick, A. Rasmussen, A. Rau, J. Rho, J. E. Rhoads, G. T. Richards, S. T. Ridgway, B. E. Robertson, R. Roskar, A. Saha, A. Sarajedini, E. Scannapieco, T. Schalk, R. Schindler, S. Schmidt, S. Schmidt, D. P. Schneider, G. Schumacher, R. Scranton, J. Sebag, L. G. Seppala, O. Shemmer, J. D. Simon, M. Sivertz, H. A. Smith, J. Allyn Smith, N. Smith, A. H. Spitz, A. Stanford, K. G. Stassun, J. Strader, M. A. Strauss, C. W. Stubbs, D. W. Sweeney, A. Szalay, P. Szkody, M. Takada, P. Thorman, D. E. Trilling, V. Trimble, A. Tyson, R. Van Berg, D. Vanden Berk, J. VanderPlas, L. Verde, B. Vrsnak, L. M. Walkowicz, B. D. Wandelt, S. Wang, Y. Wang, M. Warner, R. H. Wechsler, A. A. West, O. Wiecha, B. F. Williams, B. Willman, D. Wittman, S. C. Wolff, W. M. Wood-Vasey, P. Wozniak, P. Young, A. Zentner, and H. Zhan. LSST Science Book, Version 2.0. *arXiv e-prints*, art. arXiv:0912.0201, Dec. 2009. doi: 10.48550/arXiv.0912.0201.

[21] A. B. Newman, R. S. Ellis, and T. Treu. Luminous and Dark Matter Profiles from Galaxies to Clusters: Bridging the Gap with Group-scale Lenses. , 814(1):26, Nov. 2015. doi: 10.1088/0004-637X/814/1/26.

[22] A. Sonnenfeld, T. Treu, R. Gavazzi, S. H. Suyu, P. J. Marshall, M. W. Auger, and C. Nipoti. The SL2S Galaxy-scale Lens Sample. IV. The Dependence of the Total Mass Density Profile of Early-type Galaxies on Redshift, Stellar Mass, and Size. , 777(2):98, Nov. 2013. doi: 10.1088/0004-637X/777/2/98.

[23] S. Vegetti, S. Birrer, G. Despali, C. D. Fassnacht, D. Gilman, Y. Hezaveh, L. Perreault Levasseur, J. P. McKean, D. M. Powell, C. M. O'Riordan, and G. Vernardos. Strong gravitational lensing as a probe of dark matter. *arXiv e-prints*, art. arXiv:2306.11781, June 2023. doi: 10.48550/arXiv.2306.11781.

[24] C. K. Young and M. J. Currie. A new extragalactic distance indicator based on the surface brightness profiles of dwarf elliptical galaxies. *Monthly Notices of the Royal Astronomical Society*, 268(1):L11–L15, 1994.